TUNABLE DYNAMICS PLATFORM FOR MILLING EXPERIMENTS

Tyler Ransom, Andrew Honeycutt, and Tony L. Schmitz
Department of Mechanical Engineering and Engineering Science
University of North Carolina at Charlotte
Charlotte, NC, USA

INTRODUCTION

Time and frequency domain milling process models may be implemented to enable pre-process parameter selection for optimized performance [1]. To complete these simulations and validate the results, the system dynamics must be known. Typically, the cutting tool flexibility dominates the system dynamics, although the workpiece can introduce significant flexibility in some cases as well.

To realize a validation platform with simple (often single degree of freedom) dynamics, flexures are routinely used to support the workpiece; see Fig. 1. In this configuration, the flexure stiffness is selected to be much lower than the tool stiffness so that the tool dynamics can be effectively ignored. The experimental challenge with using flexures is that the damping is low. This can lead to unrealistic testing scenarios. In this paper, a flexure platform with tunable stiffness, natural frequency, and viscous damping is described which offers an ideal platform for milling process dynamics experiments.

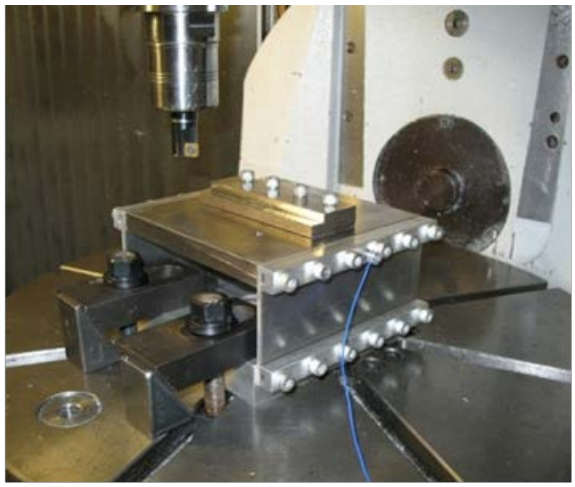

Figure 1. Parallelogram, leaf-type flexure used for milling experiments.

PLATFORM DESCRIPTION

The basis for the milling platform designed and tested in this study is a parallelogram, leaf-type flexure. By selecting the leaf geometry and workpiece/platform mass, the stiffness and natural frequency can be defined to meet the experimental requirements. The design approach is described in [2] and, for brevity, is not discussed here. As noted, however, the damping for this geometry is low.

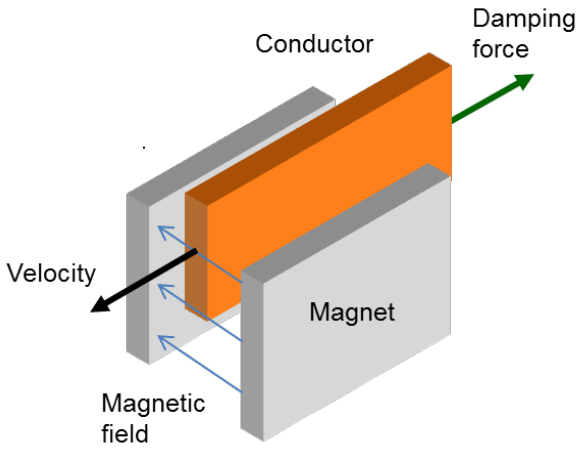

Figure 2. Schematic of an eddy current damper.

To introduce higher damping using a first principles model, the addition of an eddy current damper is proposed. The viscous (velocity-dependent) damping force for an eddy current damper can be described analytically. Figure 2 displays the motion of a conductor[1] relative to a magnet (or magnet pair) with the motion perpendicular to the magnet pole direction. The eddy current density, $\vec{J}$, depends on the conductivity, σ, and the cross product of the velocity, $\vec{v}$, and magnetic field, $\vec{B}$; see Eq. 1. The eddy current force is then calculated as the volume integral of the product of the eddy current density and the magnetic field; see Eq. 2. Mathematically, the two cross products yield a

[1] The conductor is a conductive, non-magnetic material. Aluminum and copper are common choices.

damping force which acts in the direction opposite to the velocity.

$$\vec{J} = \sigma\left(\vec{v} \times \vec{B}\right) \quad (1)$$

$$\vec{F} = \int_V \left(\vec{J} \times \vec{B}\right) dV \quad (2)$$

The damping force magnitude, *F*, is described by Eq. 3, where δ is the conductor thickness, *B* is the magnetic field strength, *S* is the magnet area, α_1 incorporates surface charge effects, α_2 incorporates end effects from the finite width conductor, and *v* is the velocity magnitude [3]. As shown, Eq. 3 can be rewritten as the product of a viscous damping coefficient, *c*, and the velocity magnitude. This viscous damping coefficient enables model-based damping prediction and selection for milling operations.

$$F = \left(\sigma \delta B^2 S\left(\alpha_1 + \alpha_2\right)\right) v = cv \quad (3)$$

The eddy current damper concept displayed in Fig. 2 was embedded inside an aluminum flexure as shown in Fig. 3. The conductor was attached to the flexure platform and two permanent magnet sets were attached to the flexure base, one on each side of the conductor. The arrangement of the eight 25.4 mm square magnets is shown in Fig. 4; aluminum screws were used to avoid disrupting the magnetic field.

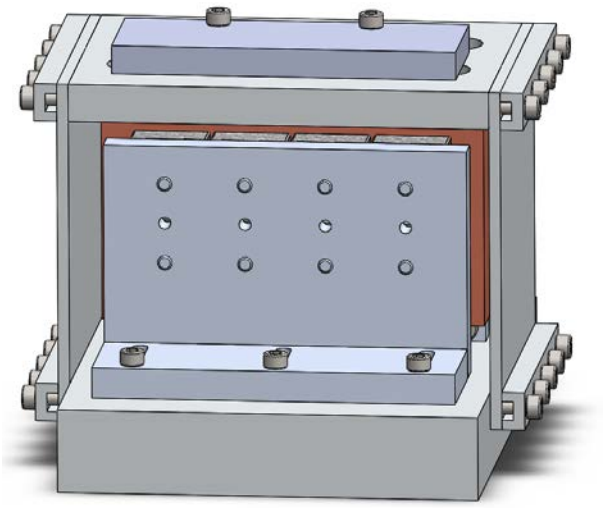

Figure 3: Flexure with embedded eddy current damper.

DAMPED FLEXURE DESIGN

The solid model displayed in Fig. 3 was constructed and tested. As shown in Eq. 3, the viscous damping coefficient can be predicted using σ, δ, *B*, *S*, and the edge effect terms, which serve to reduce the damping value; see Table 1. The conductor was a 19.1 mm thick copper plate that extended outside the magnet surface area. The magnetic field strength was measured at 64 locations over the surface of the eight permanent magnets using a gaussmeter (Integrity Design & Research Corp., IDR-329-T). Measurements were performed at a distance of 0.8 mm from the surface; this was the air gap between the magnets and conductor after assembly. The average value for all 64 measurements at the 0.8 mm distance is listed.

Table 1: Eddy current damper design parameters.

Parameter	Value
σ	5.96×10^7 A/V-m
δ	19.1 mm
B	4580 Gauss (0.458 T)
S	4.6×10^{-3} m^2
α_1*	0.352
α_2*	-0.177

*These terms were calculated using Eqs. 9 and 20, respectively, from [3].

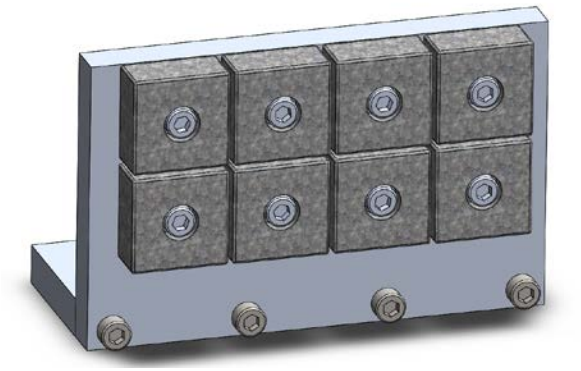

Figure 4: Permanent magnet mount.

For the values listed in Table 1, the predicted eddy current damper *c* value is 192 N-s/m. The corresponding dimensionless damping ratio, ζ, is calculated using Eq. 4, where *k* is the flexure stiffness provided in Eq. 5 and *m* is the equivalent flexure mass given by Eq. 6 [2]. In Eq. 5, *E* is the aluminum leaf's elastic modulus (69 GPa), *w* is the width (101.6 mm), *t* is the thickness (3.8 mm), and *l* is the length (88.9 mm). In Eq. 6, m_p is the combined mass of the

platform, conductor, top leaf clamps, and fasteners (2.098 kg) and m_l is the leaf mass (0.12 kg). The predicted damping ratio is 0.063 (6.3%). Using the flexure stiffness (1.093×10^6 N/m) and mass values (2.277 kg), the predicted undamped natural frequency is f_n = 110 Hz.

$$\zeta = \frac{c}{2\sqrt{km}} \tag{4}$$

$$k = 2Ew\left(\frac{t}{l}\right)^3 \tag{5}$$

$$m = m_p + 2\left(\frac{26}{35}m_l\right) \tag{6}$$

EXPERIMENTAL RESULTS

Modal tests were performed to identify the actual damping ratio for the flexure. The setup is shown in Fig. 5. An instrumented hammer was used to excite the structure and the response was measured using a low-mass accelerometer. The modal parameters extracted from the single degree of freedom frequency response function were: f_n = 110 Hz, k = 1.06×10^6 N/m, and ζ = 0.046. The disagreement in the damping ratio is attributed to approximations in the charge and edge effects.

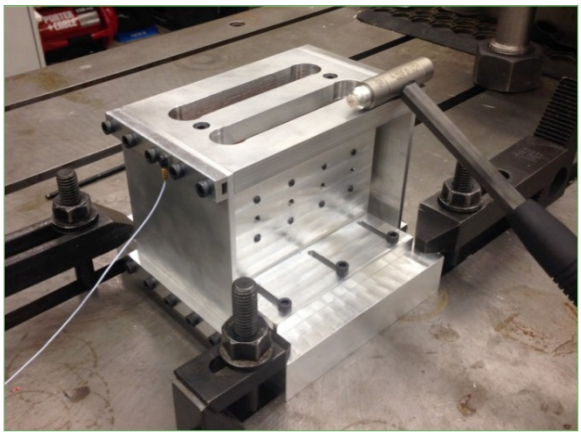

Figure 5: Impact testing setup for flexure.

Modal tests were also performed after removing the magnets so that the eddy current damping effect was eliminated, but the structure was not otherwise modified. The modal parameters extracted from the single degree of freedom frequency response function were: f_n = 108 Hz, k = 9.03×10^5 N/m, and ζ = 0.014. The addition of the eddy current damper provided a 229% increase in damping.

Given the successful fabrication and testing of the flexure, machining trials were completed to demonstrate: 1) agreement between the predicted and experimental milling stability as a function of spindle speed and axial depth of cut; and 2) the change in the stability behavior with and without the eddy current damper in place.

First, a 6061-T6 workpiece was added to the platform and modal tests were repeated for the new setup as mounted on the CNC machine table; see Fig. 6, where the accelerometer attached to the flexure was used to identify stable and unstable cutting conditions. The new modal parameters were: f_n = 110.6 Hz, k = 9.29×10^5 N/m, and ζ = 0.043 with the magnets in place and: f_n = 108 Hz, k = 9.03×10^5 N/m, and ζ = 0.015 with no magnets.

Figure 6: Milling setup showing damped flexure, two-flute endmill, and accelerometer.

For the two-flute endmill/6061-T6 aluminum workpiece, the specific cutting force was 700 N/mm^2 and the force angle was 70 deg. Using these values together with the flexure dynamics (the tool point frequency response was an order of magnitude stiffer and was ignored), stability lobe diagrams were generated for the damped and undamped flexure setups [1]. Figure 7 shows the limiting axial depth of cut (b_{lim}) as a function of spindle speed (Ω) for a 25% radial immersion up milling cut.

Two spindle speeds were selected to validate the milling stability: 2000 rpm and 3500 rpm. In both cases, the predicted increase in the limiting depth of cut with the addition of the eddy current

damper is obtained. The results are presented in Table 2. Cuts were identified as stable or unstable based on the frequency content of the accelerometer signal, A. If significant content amplitude was observed at frequencies other than the tooth passing frequency and its harmonics, the cut was considered unstable. The chatter frequency was verified to be near the flexure natural frequency in each case.

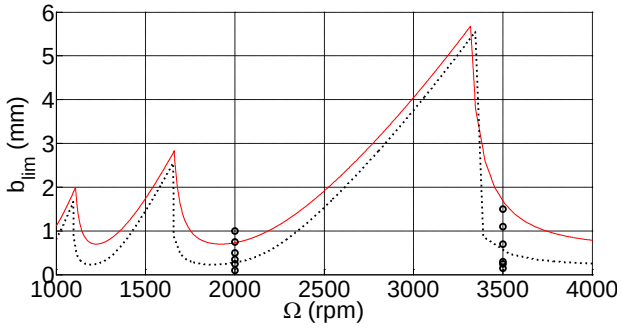

Figure 7: Stability limit with magnets (solid) and without magnets (dashed). The test points from Table 2 at 2000 rpm and 3500 rpm are marked by circles.

Table 2: Stability testing results. U indicates the undamped flexure and D indicates the damped flexure. Stable = o, unstable = ×, marginal = m.

2000 rpm			3500 rpm		
b (mm)	U	D	b (mm)	U	D
0.1	o	o	0.15	o	o
0.25	m	o	0.25	m	o
0.35	x	o	0.3	x	o
0.5	x	o	0.7	x	o
0.75	x	m	1.1	x	o
1.0	x	x	1.5	x	x

Accelerometer frequency content examples are provided for the undamped flexure at a spindle speed of 3500 rpm in Fig. 8 (0.15 mm axial depth) and Fig. 9 (0.7 mm). In Fig. 8, content at the tooth passing frequency (116.7 Hz) and its multiples (as well as the runout frequencies) is observed. This cut is stable. In Fig. 9, on the other hand, the signal amplitude is 30 times larger with the dominant peak near the flexure natural frequency. This cut exhibited chatter.

CONCLUSIONS

This study described a new approach for prescribing the structural dynamics in machining stability testing. It demonstrated a passive platform with tunable dynamics that can be selected at the design stage. The design process was detailed so that other researchers can implement the new strategy.

REFERENCES

[1] Schmitz T, Smith, S (2009) Machining Dynamics: Frequency Response to Improved Productivity. Springer, New York, NY.

[2] Smith, S (2000) Flexures: Elements of Elastic Mechanisms. CRC Press, London, UK.

[3] Bae, JS, Moon, KK, Inman, D (2005) Vibration suppression of a cantilever beam using eddy current damper. Journal of Sound and Vibration 284:805-824.

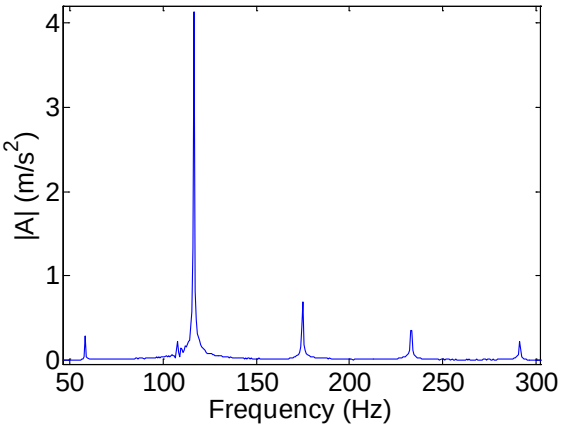

Figure 8: Stable cut at 0.15 mm axial depth and 3500 rpm spindle speed for the undamped flexure.

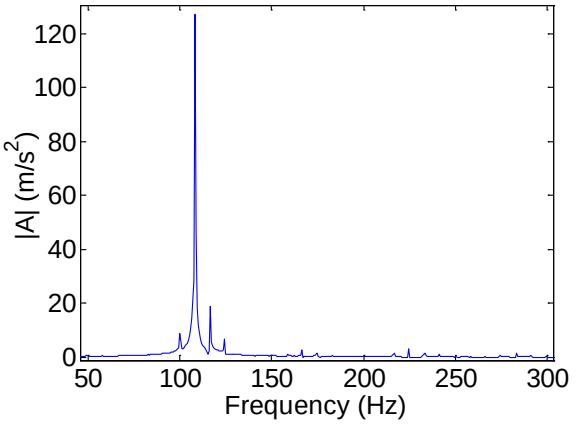

Figure 9: Unstable cut at 0.7 mm axial depth and 3500 rpm spindle speed for the undamped flexure.